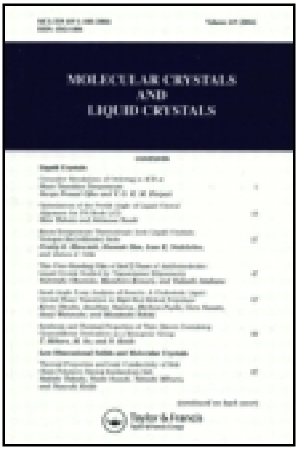

Molecular Crystals and Liquid Crystals
Publication details, including instructions for authors and subscription information:
http://www.tandfonline.com/loi/gmcl16

Triple Hysteresis Loop of a Ferroelectric Liquid Crystal

Shoichi Kai [a], Tetsuya Hashimoto [a], Ko Ose [a] & Mashahide Imasaki [a]

[a] Department of Electrical Engineering, Kyushu Institute of Technoloyg Tobato, Kitakyushu, 804, Japan

Version of record first published: 20 Apr 2011.

Mol. Cryst. Liq. Cryst., 1985, Vol. 130, pp. 143–162
0026-8941/85/1302-0143/$20.00/0

Printed in the United States of America

Triple Hysteresis Loop of a Ferroelectric Liquid Crystal

SHOICHI KAI, TETSUYA HASHIMOTO, KO OSE and MASAHIDE IMASAKI

Department of Electrical Engineering, Kyushu Institute of Technology, Tobata Kitakyushu, 804 Japan

(*Received January 16, 1985*)

A triple hysteresis loop, which was quite different from that of ferrielectricity, was first observed in a ferroelectric liquid crystal with positive dielectric anisotropy. In the ferrielectric case, the direction of the field-induced polarization is the same as that of the original one. On the contrary, it was an inverse direction to that in the present case. When the temperature was near the phase transition point from smectic A to smectic C* and/or when the applied electric field was sufficiently large, the triple hysteresis loop was easily observed. The temperature dependence of the threshold field for the triple hysteresis loop was analogous to that for electrohydrodynamic instability (EHDI) in smectic C. A similar additional loop to that of the triple hysteresis loop was also observed in the D-E hysteresis loop of MBBA in a very high field. On the basis of these experimental facts, the triple loop is explained by EHDI.

1. INTRODUCTION

It has been said that the D-E hysteresis loop in ferroelectric liquid crystals resulted from the pinning of helicoidal structures.[1] The true origin, however, is still unknown. It can be said that there are two types of dielectric hysteresis with different responses[2] (~sec and ~msec), which may come from different origins, respectively. These two mechanisms have often been confused. Many experimental facts (polarization reversal, change of light transmittance, electric field, frequency dependence of the polarization, etc.) are not yet perfectly explained. The present authors, therefore, are studying the dielectric properties of ferroelectric liquid crystals to make the origin clear.

A clear triple hysteresis loop was first observed in $RbLiSO_4$ by Shiroishi et al.[3] and they concluded that it was caused by ferrielectricity, simultaneously considering the results of X-ray structure analysis. A triple hysteresis loop was also observed in a ferroelectric liquid crystal with positive dielectric anisotropy but it was quite different from the one of $RbLiSO_4$. In the case of $RbLiSO_4$, a field-induced transition produced a polarization of the same direction as the original one but in the present case it was the inverse. When the sample temperature was near the phase transition point from smectic A to smectic C* and/or when sufficiently high voltage was applied to the sample, the triple hysteresis loop easily appeared. We studied the temperature and the electric field dependence of this new nonlinear phenomenon.

2. EXPERIMENTAL

We used DOBAMBC (p-n-decyloxybenzilidene-p′-amino-2-methylbutyl cinnamate), which exists in the smectic C* phase from 63 to 95°C, as a ferroelectric liquid crystal. The sample was sandwiched between two nesa-coated glass plates. Mylar spacers were used in order to define the sample thickness, which was confirmed by the capacitance method and by measurement through a microscope. No treatment was given to the nesa-coated glass plates but they were thoroughly cleaned by aceton and distilled water. The sample thickness used in this study was 30~50 μm. The cell was placed in a hotstage. The temperature of the sample was measured by a plutinum resistance thermometer, GB 100-2 (Sōgo Electric Co.), and regulated to better than 0.01°C by a controller (artronix 5350). To obtain a good homogeneous alignment, the sample was slowly cooled (2~3° C/h) from the isotropic to the smectic A phase. The triple hysteresis loop was studied by the Pepinsky bridge[4] using a 60 Hz a.c. power supply. All signals were recorded onto a magnetic disk and evaluated by a signal analyser (Iwatsu SM-2100A). This analyser is capable of X-Y transformation of signals, compensation of a phase and enlargement of signals by any magnification.

3. ELECTRIC FIELD DEPENDENCE OF D-E LOOP

At first, we define:

E^* : the threshold field for the additional loop,

E_m : the maximum instantaneous field,

P_{V1} : variation of the polarization in the same direction as the original one,

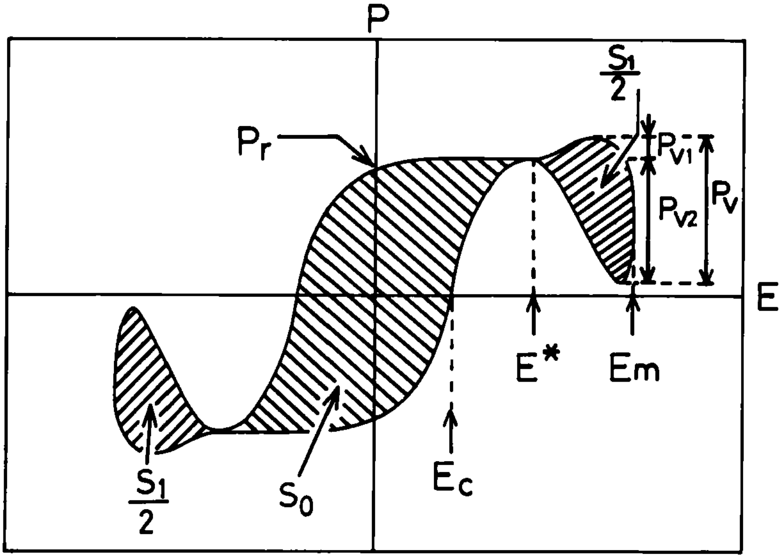

FIGURE 1 Schematic diagram of triple hysteresis loop. P_r: remanent polarization, P_{V1}: variation of polarization in the same direction as the original one, P_{V2}: that in the inverse direction to the original one, P_V: total variation of polarization in the additional loop (= P_{V1} + P_{V2}), E_c: coercive field, E*: threshold field for the additional loop, E_m: maximum instantaneous field, S_0: power loss (= area) due to the original loop, S_1: that due to the additional loop.

P_{V2} : that in the inverse direction to the original one,
P_V : total variation of the polarization in the additional loop (= P_{V1} + P_{V2}),
S_0 : power loss due to the original loop,
S_1 : that due to the additional loop,

respectively, as shown in Figure 1. One should note here that the additional loop cannot be compensated by a resistance of the bridge, unlike a loop frequently observed at uncompensation. In order to make sure whether the triple hysteresis loop is an intrinsic phenomenon or not, polarization reversal was also studied by the electric field of a triangular wave.[5] This result is shown in Figure 2. The induced current shows a slow decrease, which corresponds to the polarization reversal due to the additional loop, after the sharp increase of that due to the original loop. The D-E hysteresis loop of the triangular wave is shown in Figure 3. It is almost the same as that of the sinusoidal wave, which is shown in Figure 1, except for the somewhat larger additional loop (see also Figure 4(b)-2). It can be, therefore, concluded that the triple hysteresis loop is an intrinsic

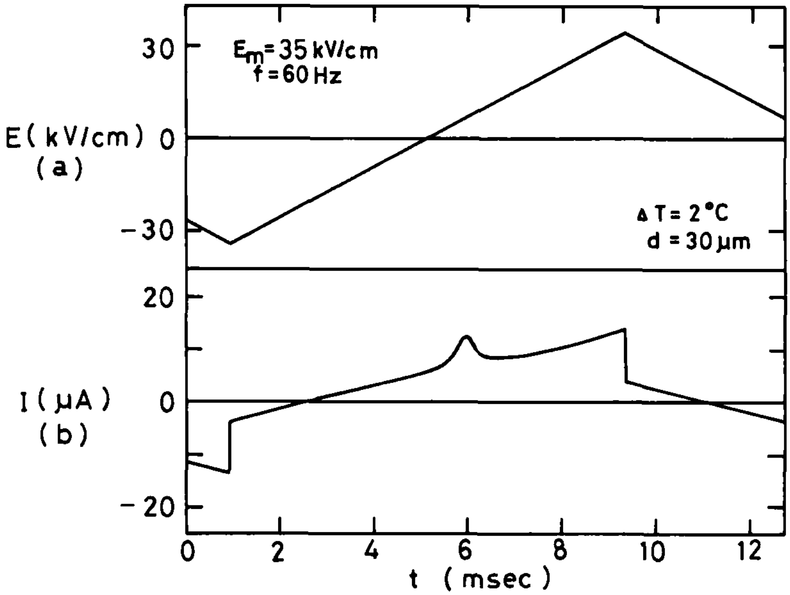

FIGURE 2 Polarization reversal for the applied electric field of a triangular wave: (a) applied voltage of the triangular wave, (b) induced current.

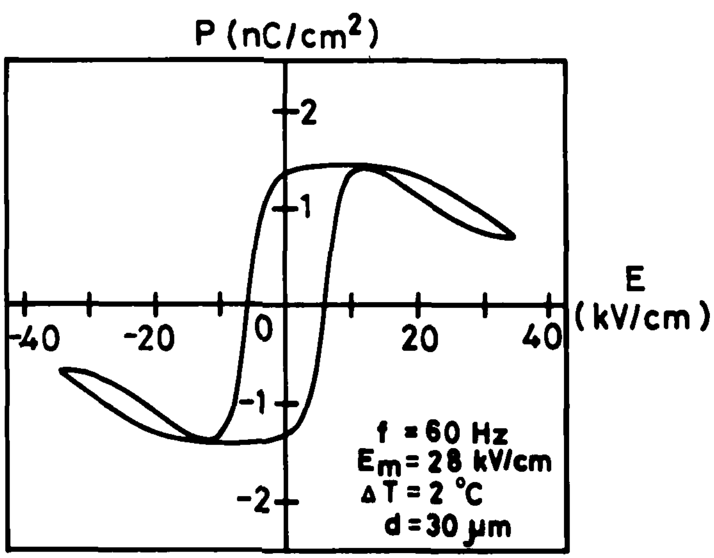

FIGURE 3 D-E hysteresis loop for the applied electric field of the triangular wave. f = 10 Hz, ⟨E⟩ = 20 kV/cm, ΔT = 2°C, d = 30 μm.
⟨E⟩ : effective electric field.

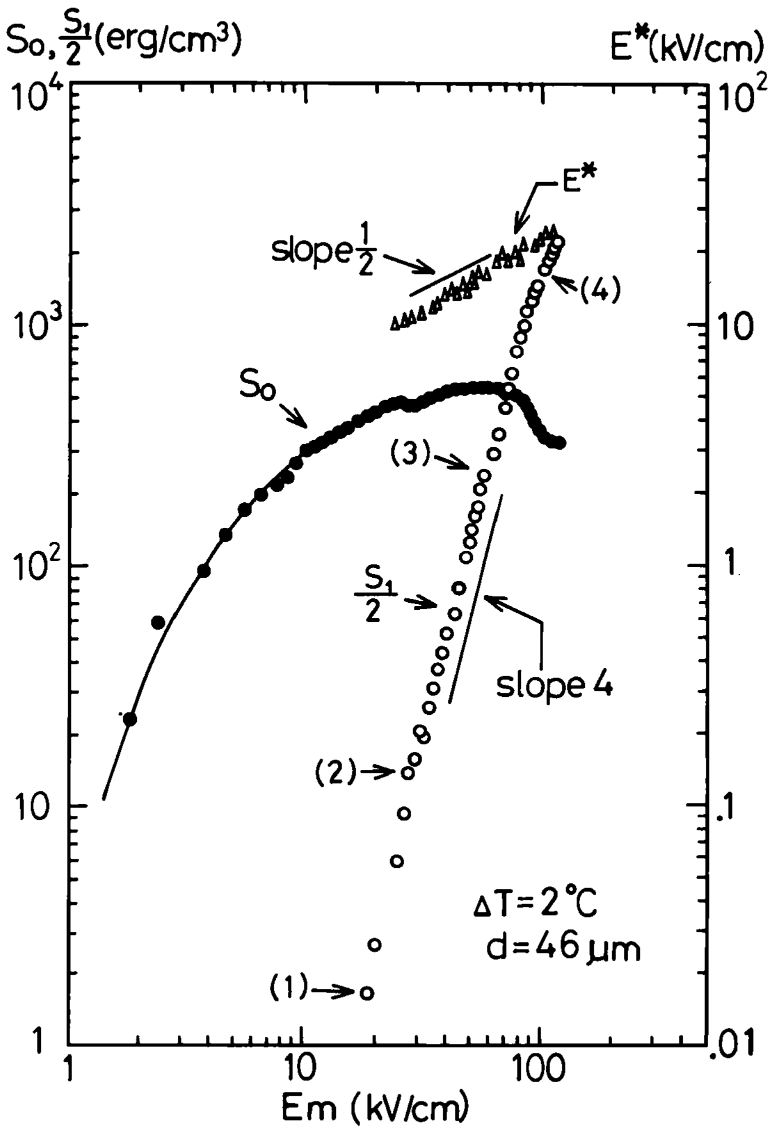

(a)

FIGURE 4 Electric field dependence of the power losses, the threshold field and the shape of the triple hysteresis loops: (a) the S_0, $S_1/2$ and E* as a function of the applied field, (b) variation of the triple hysteresis loops with an increase in the applied field; (1) ⟨E⟩ = 13 kV/cm, (2) 17.2, (3) 35, (4) 72. f = 60 Hz, ΔT = 2°C, d = 46 μm.

The triple hysteresis loops indicated by the number in Figure 4(a) are shown in Figure 4(b) of the corresponding number. $\Delta T = T_c - T$, T_c: the phase transition temperature from smectic A to smectic C*, T: the sample temperature.

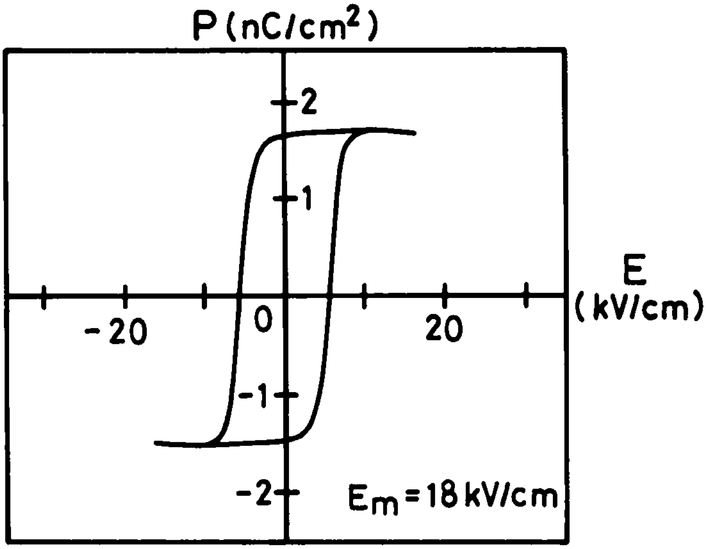

(1)

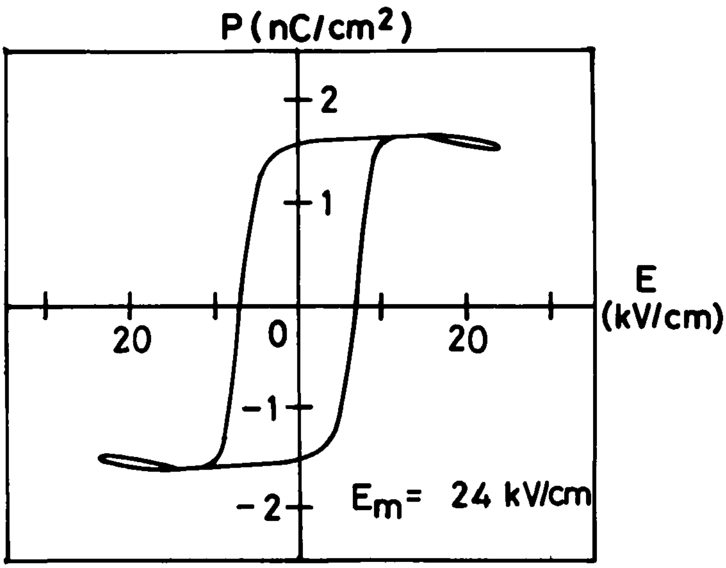

(2)

FIGURE 4 (b)—*Continued*

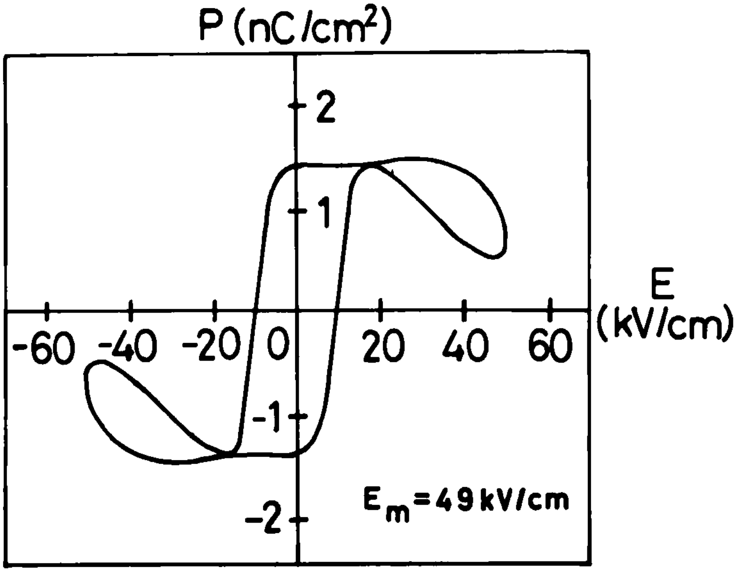

(3)

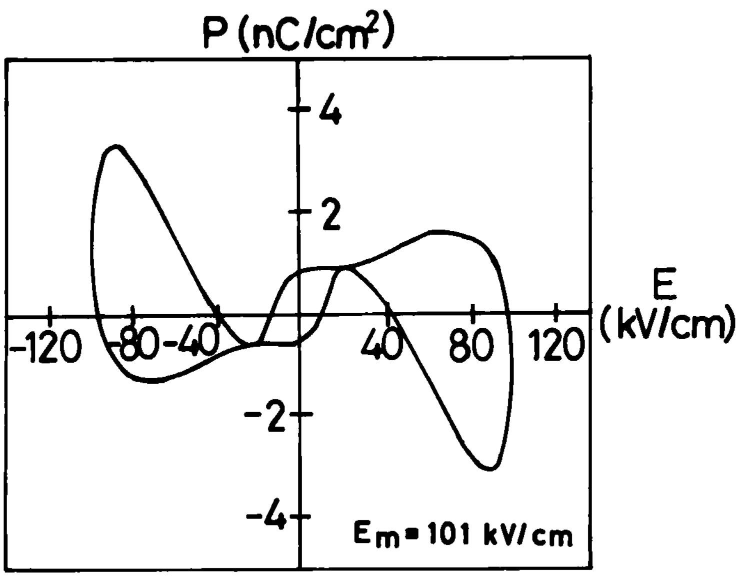

(4)

FIGURE 4 (b)—*Continued*

phenomenon and it does not result from an uncompensation of a resistance in the bridge. The electric field dependence of the S_0, $S_1/2$ and E* are summarized in Figure 4(a). The shape of the triple hysteresis loop changed with an increase of the applied field as shown in Figure 4(b). The numbers in Figure 4(a) indicate the corresponding points of the figures in Figure 4(b) which show the shapes of the loops. The S_0 of (3) in Figure 4(b) seems to be smaller than that of (2) but actually the former is larger than the latter, as can be seen from Figure 4(a). The S_0 gradually increases with an increase of the applied field and becomes maximum around 50 kV/cm. The $S_1/2$ is proportional to E_m^4 and the E* is proportional to $E_m^{1/2}$. This relation shows that the width of the additional loop increases with an increase of the applied field. It should be noted that magnitude of the reduced polarization becomes larger than that of the original one as shown in (4) of Figure 4(b). This cannot result from a disorder but suggests rather the existence of some order antiparallel to that of the original one. The electric field dependence of the $S_0 + S_1$ and the total power loss due to the triple hysteresis loop is shown in Figure 5. It indicates a sharp increase around 50 kV/cm at which S_0 takes the maximum value. The coercive field E_c and remanent polarization P_r are also shown as a function of the electric field in Figures 6(a) and (b). As the applied field increases, the E_c increases monotonically but the P_r starts to decrease above saturation like regime around 20 kV/cm. The former is seen to resemble that of solid state ferroelectrics[6] but the latter is different from them. The latter suggests the appearance of factors which reduce the polarization by increasing the applied field. An increase of the E_c and a decrease of the P_r in Figure 6 lead the maximum of the S_0 in Figure 4(a) since $S_0 \sim 2P_rE_c$. The electric field dependence of the $P_{V1} + P_V$ is shown in Figure 7. It is interesting that the saturation phenomenon can be seen in the $P_{V1} + P_r$ in contrast with the P_r. The $P_V/(P_{V1} + P_r)$ is proportional to $E_m^{2.6}$ as shown in Figure 8. The width of the additional loop can be considered to increase in proportion to E_m in a very high field since the E* becomes negligibly smaller compared with E_m. The S_1 is proportional to E_m^4 but the rectangular area of the product width and the P_V (S_2) is proportional to $E_m^{3.6}$. This difference of exponents is caused by an increase of the occupation ratio of the loop: $S_1/2S_2$, with an increase of the applied field.

4. TEMPERATURE DEPENDENCE OF D-E LOOP

The temperature dependence of the S_0 and $S_1/2$ at the constant field of $E_m = 14.1$ kV/cm ($\langle E \rangle = 10$ kV/cm) are shown in Figure 9. When

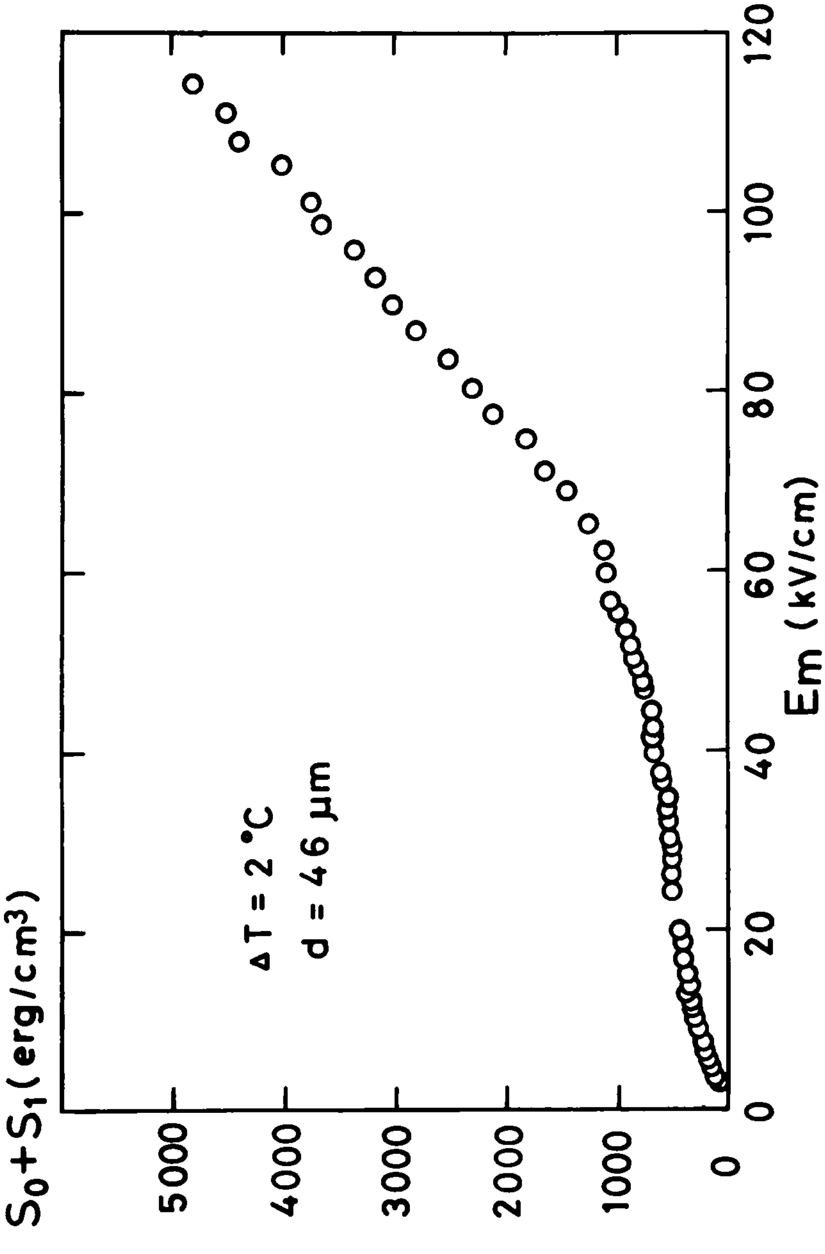

FIGURE 5 Electric field dependence of the $S_0 + S_1$. $f = 60$ Hz, $\Delta T = 2$°C, $d = 46$ µm.

(a)

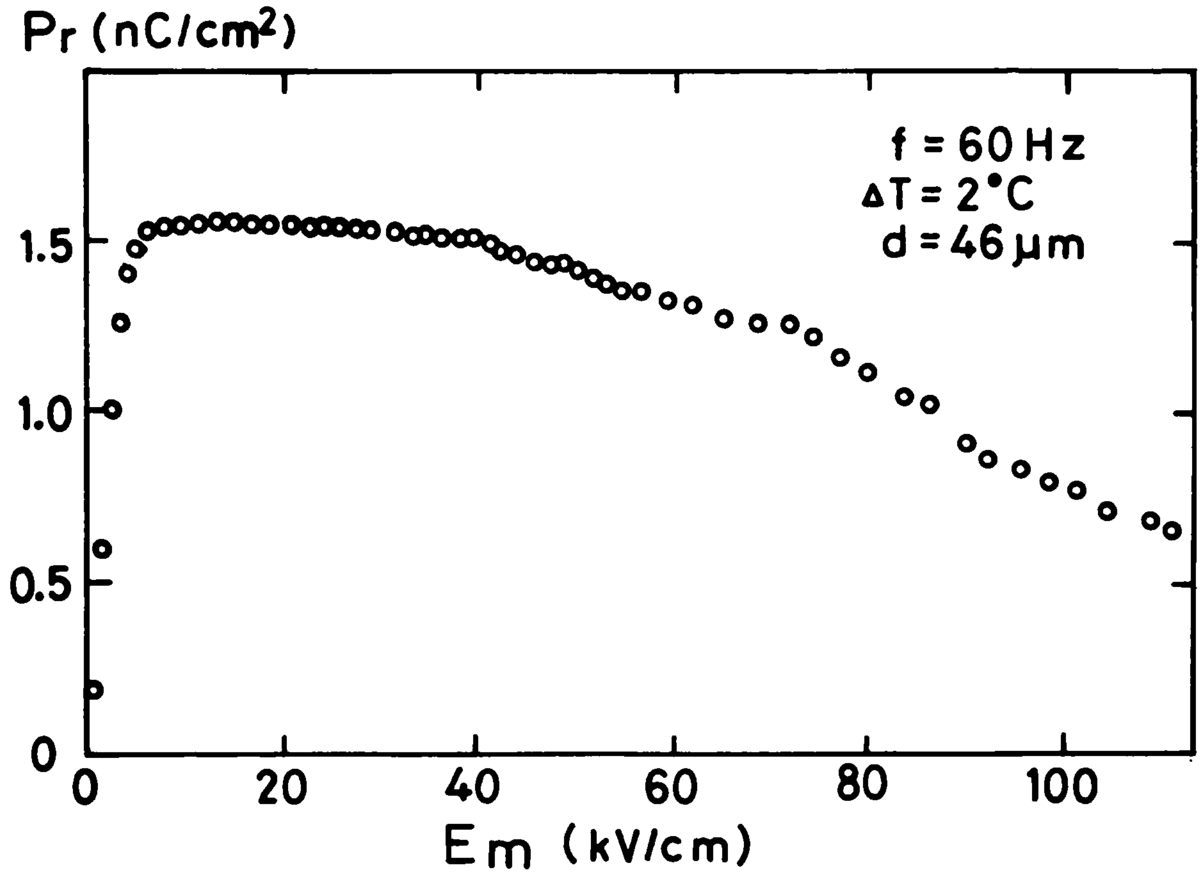

FIGURE 6 Remanent polarization P_r and coercive field E_c as a function of the applied field: (a) remanent polarization P_r, (b) coercive field E_c. $f = 60$ Hz, $\Delta T = 2°C$, $d = 46\ \mu m$.

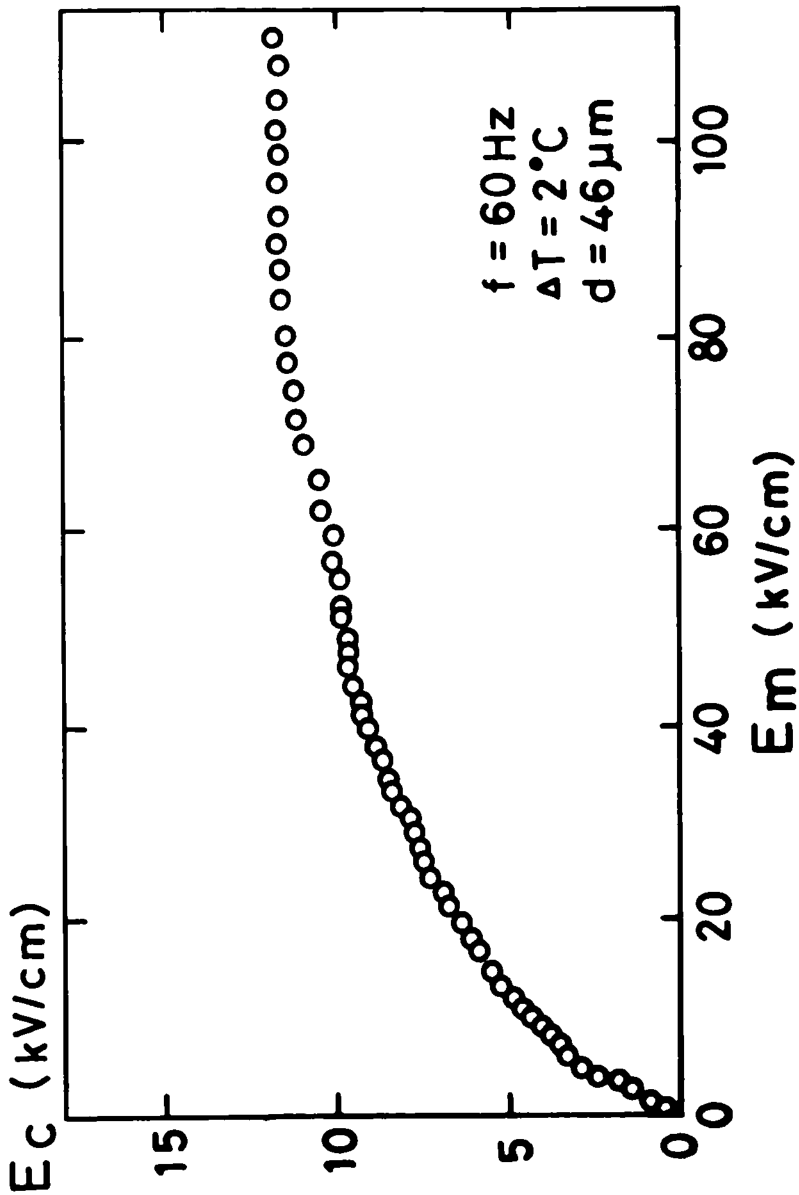

(b)

FIGURE 6—*Continued*

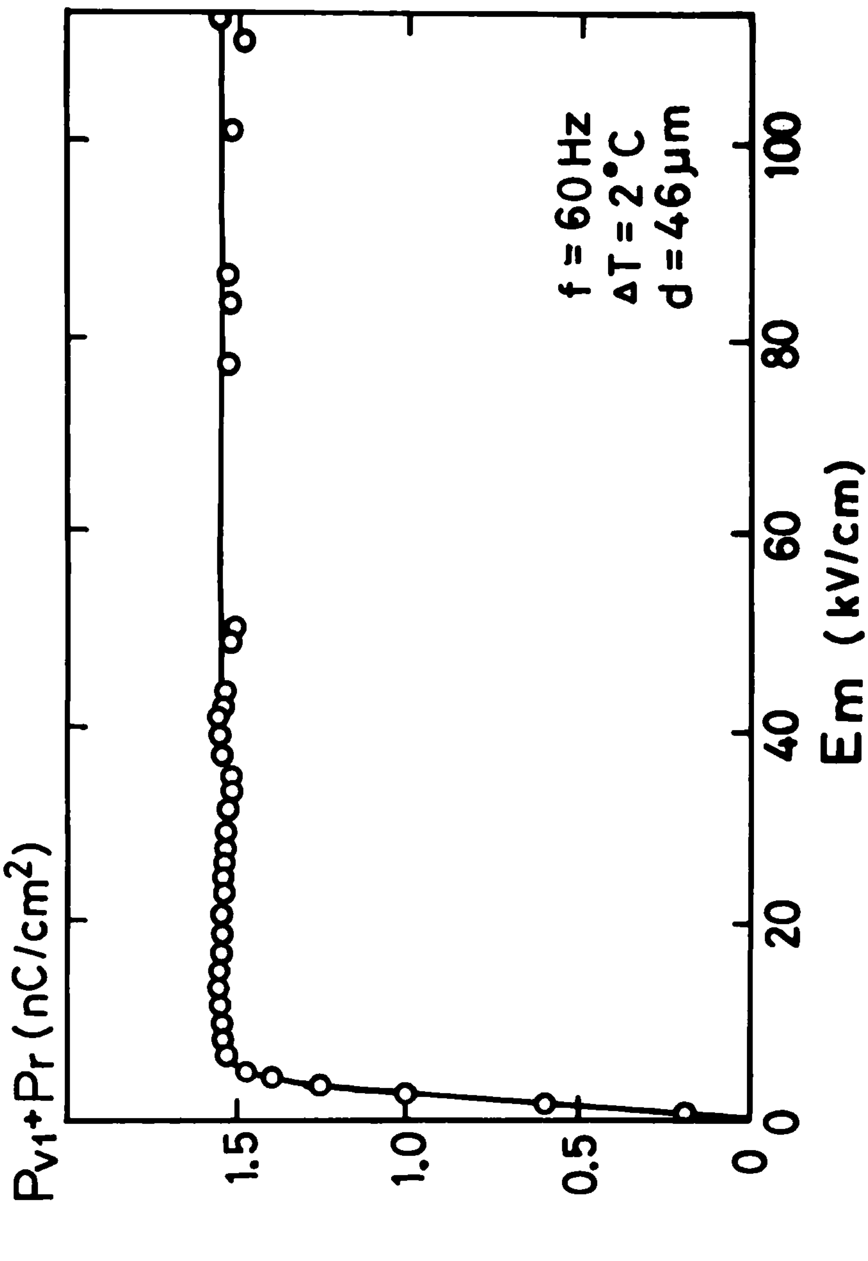

FIGURE 7 Electric field dependence of the $P_{V1} + P_r$. f = 60 Hz, ΔT = 2°C, d = 46 μm.

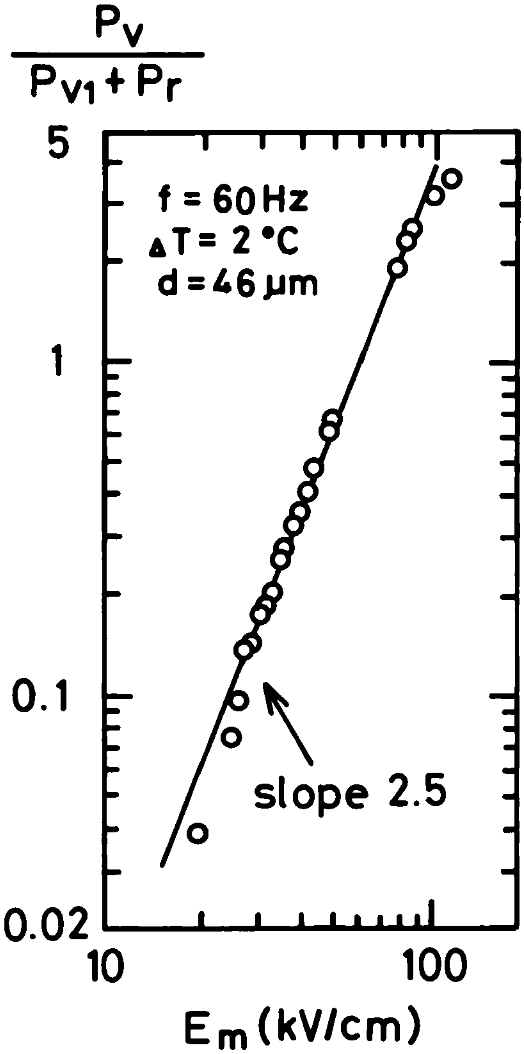

FIGURE 8 Electric field dependence of the $P_V/(P_{V1} + P_r)$. f = 60 Hz, ΔT = 2°C, d = 46 μm.

the sample temperature is lowered, the S_0 increases but the $S_1/2$ decreases. The temperature dependence of the S_0 is natural because both P_r and E_c increases as the temperature is lowered in the smectic C* phase. The temperature dependence of the $S_1/2$ indicates that the triple hysteresis loop is made difficult to appear with a decrease in temperature. The threshold electric field E_t (to obtain the triple hys-

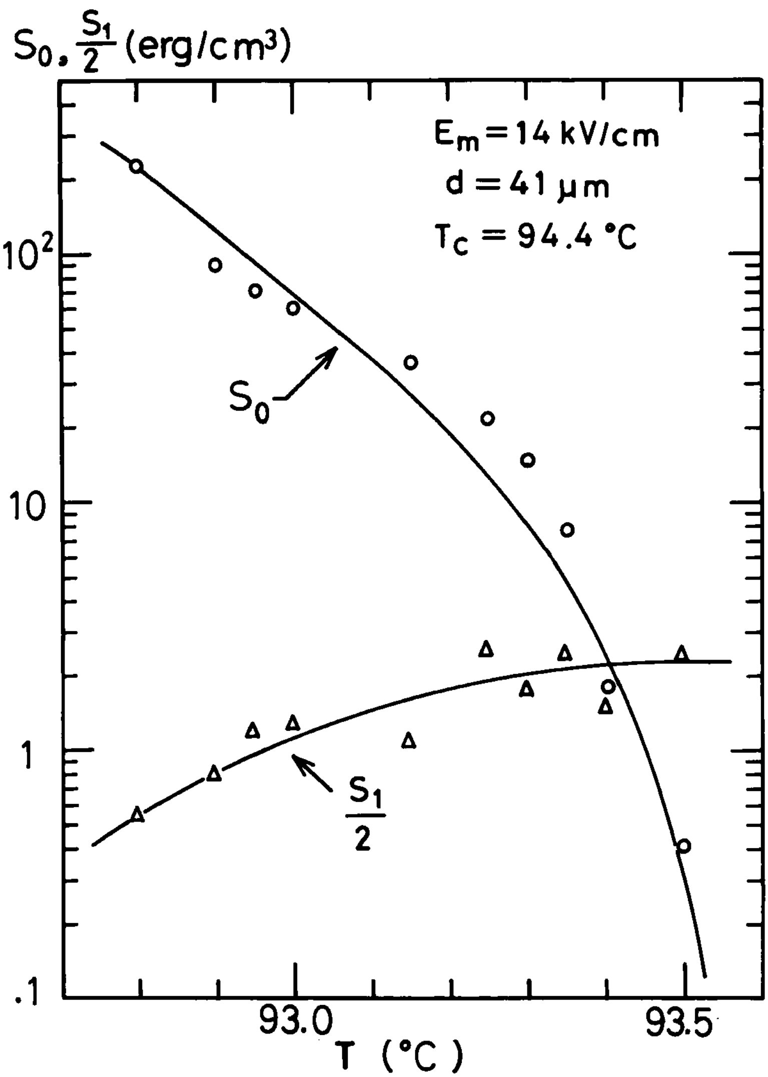

FIGURE 9 Temperature dependence of the S_0 and $S_1/2$. f = 60 Hz, ⟨E⟩ = 10 kV/cm, d = 46 μm, ΔT = 94.4°C.

teresis loop) was studied as a function of temperature and this result is shown in Figure 10. The variation of E_t with the temperature is similar to that of the rotational viscosity coefficient near the phase transition temperature from smectic A to smectic C*[7,8] and similar to that of the coercive field near the phase transition temperature from smectic C* to smectic H.[9]

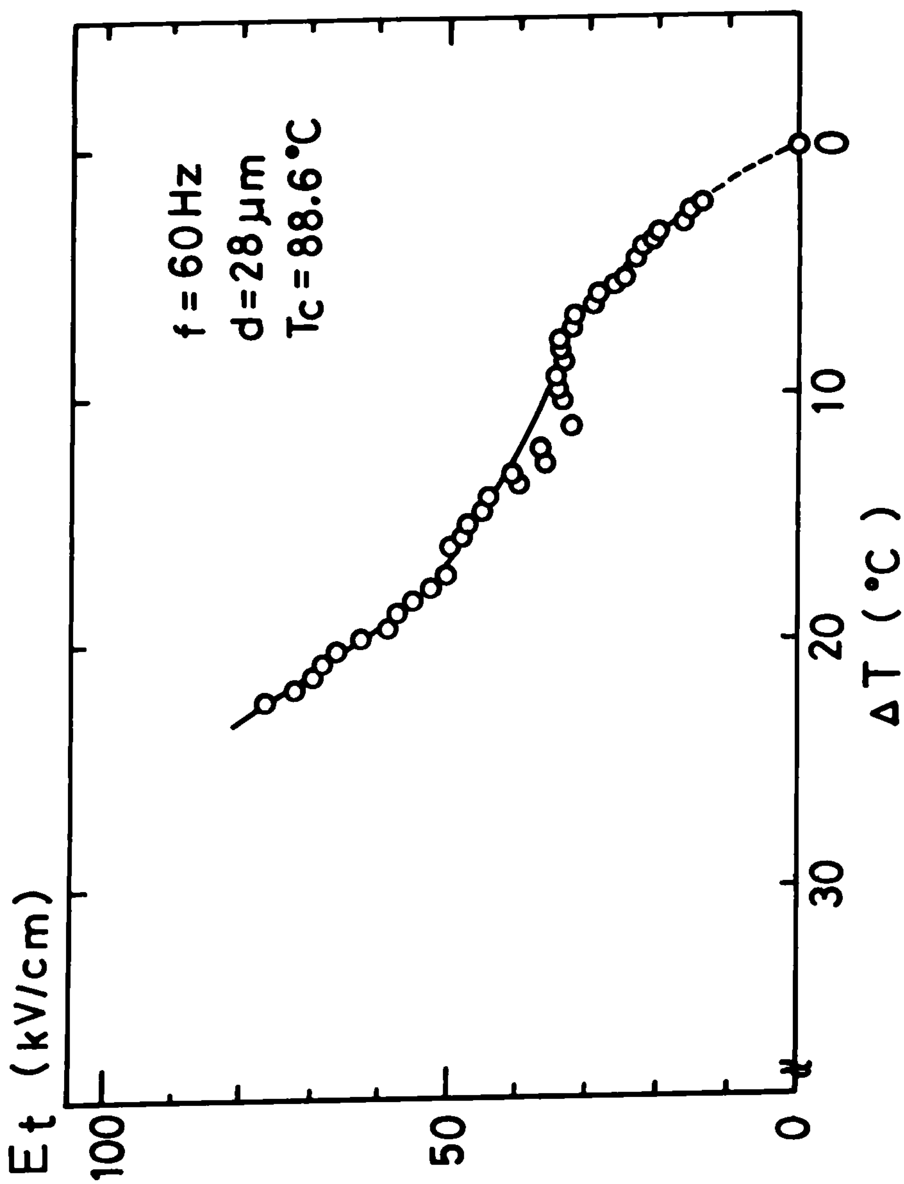

FIGURE 10 Temperature dependence of the threshold field E_t for the triple hysteresis loop. f = 60 Hz, d = 28 μm, T = 88.6°C.

5. D-E HYSTERESIS LOOP OF MBBA

In order to make clear the origin of the triple hysteresis loop, that of MBBA (N-(p-methoxybenzylidene)-p-butylaniline) in a high field was studied using a 60 Hz a.c. power supply. This result is shown in Figure 11 with the corresponding result of DOBAMBC and the time variation of their X and Y components. In Figure 11(a), we can see two loops, which correspond to the additional loop in the triple hysteresis loop. Both reduced and enhanced polarization are also observed in these two loops. The time variation of the Y component in MBBA shows hollows, which correspond to the additional loop in the D-E hysteresis loop, like that of DOBAMBC. The variation of the polarization in Figure 11(a): P_A was studied as a function of the applied field and this result is shown in Figure 12. The electric field dependence of the P_A in MBBA is the same as that of $P_V/(P_{V1} + P_r)$ in DOBAMBC, which is shown in Figure 6. It is considered, therefore, that both P_V and P_A are caused by the same mechanism. In the nematic phase of MBBA, electrical conductivity decreases above a threshold field with an increasing field at such a high field,[10] because of a parametric oscillation of the nematic director in a turbulent flow of electrohydrodynamic instability (EHDI).[10-13] Two loops of MBBA may be, therefore, caused by this nonlinear conductivity change.

6. SUMMARY AND DISCUSSION

We have found the following experimental facts about the triple hysteresis loop;

(1) As the additional loop has never been compensated by a resistance of the bridge, it is an intrinsic phenomenon in a ferroelectric liquid crystal.

(2) A triple hysteresis loop consists of an original loop and two additional ones with inverse polarization.

(3) A power loss due to the additional loop increases much more than that of the original loop with an increase of the applied field.

(4) Reduced and enhanced polarization can be observed in the additional D-E loop.

(5) Polarization of the original loop indicates a sharp change in the coercive field but that of the additional loop shows a rather gentle change above the threshold field E_t for the triple loop.

(6) It is easy to observe triple hysteresis loops near the phase transition temperature T_c and/or in a very high field. Near T_c, both

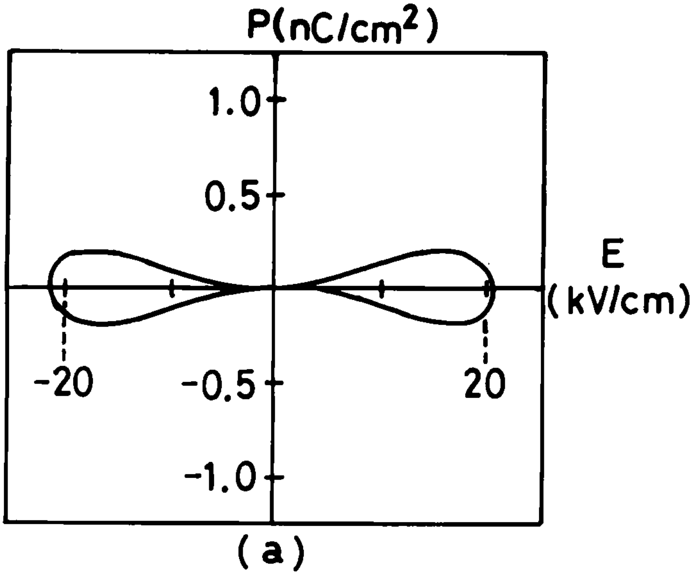

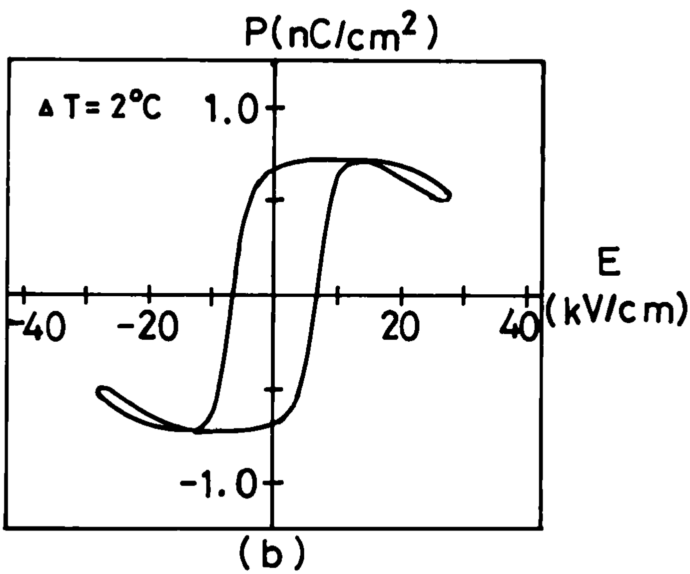

FIGURE 11 D-E hysteresis loops and time variation of their X and Y components for a sinusoidal wave: (a) D-E hysteresis loop of MBBA (N-(p-methoxybenzylidene)-p-butylaniline); f = 60 Hz, T = 32.19°C, d = 100 μm, ⟨E⟩ = 15 kV/cm, (b) D-E hysteresis loop of DOBAMBC; f = 60 Hz, ΔT = 2°C, d = 30 μm, ⟨E⟩ = 20 kV/cm, (c) applied electric field (X component of the D-E loop), (d) time variation of Y component for the D-E loop of (a), (e) time variation of Y component for the D-E loop of (b).

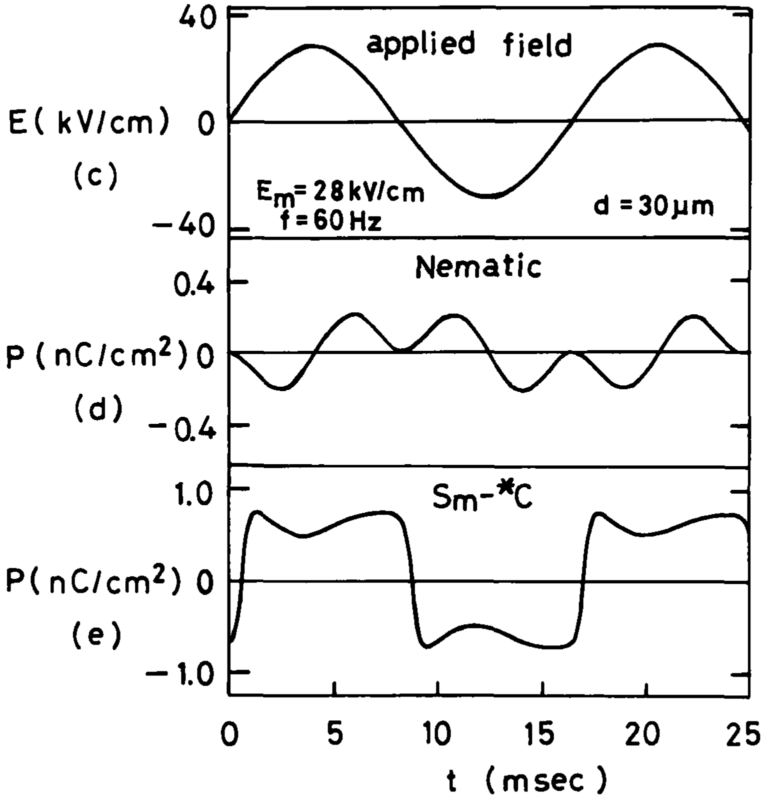

FIGURE 11—*Continued*

spontaneous polarization P_s and rotational viscosity coefficient become low but the dielectric anisotropy is virtually invariant.

(7) Two loops which correspond to the additional loop in the D-E hysteresis loop of DOBAMBC were observed in that of MBBA in a very high field and it is explained by a nonlinear conductivity change due to EHDI, including the parametric oscillation of the director in the nematic phase.[10,11]

We will try to make clear the origin of such a triple hysteresis loop from these summaries.

The EHDI in the smectic C phase has been studied mostly in HOBA (p-n-heptyloxybenzoic acid) with negative dielectric anisotropy and a positive conductive anisotropy by many authors.[14-19] Petrov et al.[19] explained the initial domains by periodic bend-twist instability, coupled with the hydrodynamic flow and the fundamental

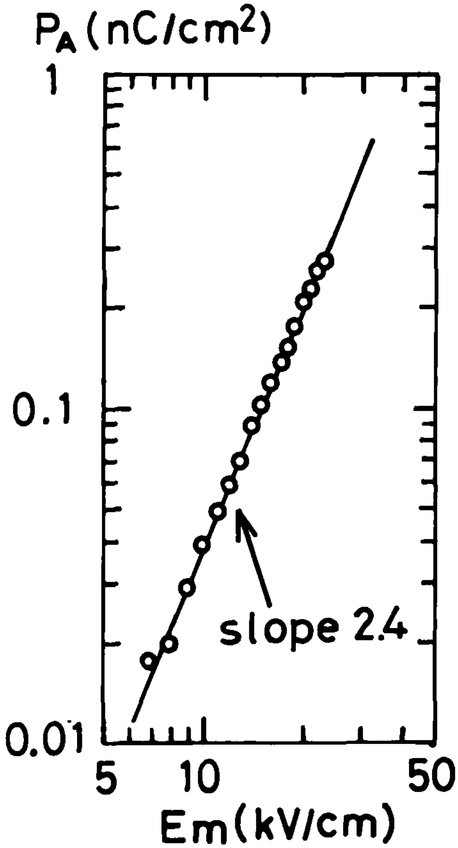

FIGURE 12 Electric field dependence of the P_A in MBBA. f = 60 Hz, T = 32.19°C, d = 100 μm.

domains by that of bend instability. Temperature dependence of the threshold field for the triple hysteresis loop is analogous to that of EHDI in smectic C. Moreover, the electric field dependence of the P_V in DOBAMBC is the same as that of the P_A in MBBA, which is caused by EHDI.

The EHDI is classified into two types; one is the EHDI in the conduction regime, which responds within several seconds, and the other is the parametric director oscillation in the dielectric regime, which can follow any applied frequency as far as a sufficiently high field is applied. Both EHDI coexist in high fields. The alignment of the director is disturbed in the azimuthal direction by the turbulent flow of the EHDI in DOBAMBC and results in the decrease of the

P_r as shown in Figure 6. In addition to the effects of the EHDI, the director may be also modified by the dielectric interaction with the applied field as Dmitrienko et al.[20] clarified. The oscillating director, which is caused by the forced parametric oscillation in the EHDI,[11,12] may lead to nonlinear responses of conductivity and dielectricity to the applied field. These nonlinear responses are the main causes of the additional loop of the triple hysteresis loop. In the present experiment, the P_r starts to decrease around 14 kV/cm, which is lower than the lowest threshold field for the additional loop ($\sim$ 28 kV/cm) as shown in Figure 4. This experimental fact supports the idea proposed above, since the EHDI in the conduction regime starts at a lower field than the parametric director oscillation. As the threshold field for the triple hysteresis loop is determined by a competition among dielectric, ferroelectric, elastic and viscous interaction, it is easy to observe the additional loop under the condition (6) described above.

References

1. R. B. Meyer, *Mol. Cryst. Liq. Cryst.*, **40**, 33 (1977).
2. S. Kai, Y. Narushige, R. Fujimoto and M. Imasaki, *Ferroelectrics*, **58**, 255 (1984).
3. Y. Shiroishi and S. Sawada, *J. Phys. Soc. Jpn.*, **46**, 148 (1979).
4. S. Sawada, Denkitekisokutei (Electrical Measurements) eds. S. Iida et al. (Asakurashoten, Tokyo, 1966) p. 156 (In Japanese).
5. K. Miyasato, S. Abe, H. Takezoe, A. Fukuda and E. Kuze, Jpn. *J. Appl. Phys.*, **22**, L-661 (1983).
6. C. F. Pulvari and W. Kuebler, *J. Appl. Phys.*, **29**, 1315 (1958).
7. C. Rosenblatt, R. B. Meyer, R. Pindak and N. A. Clark, *Phys. Rev. A*, **21**, 140 (1980).
8. W. Kuczyński, Ber. Bunsenges. *Phys. Chem.*, **85**, 234 (1981).
9. J. Hoffmann, W. Kuzyński and J. Malecki, *Mol. Cryst. Liq. Cryst.*, **44**, 287 (1978).
10. T. Kai, S. Kai and K. Hirakawa, Tech. Rep. Kyushu Univ., 50, 445 (1977) (in Japanese) and *J. Phys. Soc. Jpn.*, **43**, 717 (1977).
11. H. Yayama, M. Takata, S. Kai and K. Hirakawa, *Tech. Rep. Kyushu Univ.*, **52**, 627 (1979) (in Japanese).
12. I. W. Smith, Y. Galerne, S. T. Lagerwall, E. Dubois-Viollette and G. Durand, *J. Physique*, **36**, C1-237 (1975).
13. S. Kai and K. Hirakawa, *Prog. Theor. Phys. Suppl.*, **64**, 212 (1978).
14. L. K. Vistin and A. P. Kapustin, *Soc. Phys.-Crystallogr.*, **13**, 284 (1968).
15. M. Gosianski, *Philips Res. Rep.*, **30**, 37 (1975).
16. S. Sakagami, A. Takase and M. Nakamizo, *Chem. Phys. Lett.*, **38**, 547 (1976).
17. P. Simova, M. Petrov and N. Kirov, *Mol. Cryst. Liq. Cryst.*, **42**, 295 (1977).
18. B. Petroff, M. Petrov, P. Simova and A. Angelov, *Ann. Phys.*, **3** 331 (1978).
19. M. Petrov and G. Durand, *J. Physique Lett.*, **42**, L-519 (1981).
20. V. E. Dmitrienko and V. A. Belyakov, *Sov. Phys. JETP.*, **51**, 787 (1980).